DYNAMICS OF THE MOLTEN CONTACT LINE

Ain A. Sonin[1] (speaker), Gregg Duthaler[2], Michael Liu[2], Javier Torresola[2]
and Taiqing Qiu[3]

OBJECTIVES

The moving molten contact line plays a key role in a number of applications, including certain coating processes, spin casting of metals, and various droplet based manufacturing techniques. The purpose of our program is to develop a basic understanding of how a molten material front spreads over a solid substrate that is below its melting point, arrests, and freezes. We are concerned particularly with the dynamic contact line that occurs in molten droplet deposition on cold substrates. Our hope is that the work will provide a scientific knowledge base for certain new applications, such as the "printing" of arbitrary three-dimensional objects by precise deposition of individual molten microdrops (Gao & Sonin, 1994), and at the same time contribute generally to the understanding of low Bond number, capillarity-driven liquid dynamics problems.

The main obstacle to progress at this time is our lack of knowledge of the basic processes in molten droplet deposition. We do not yet know the basic laws that govern the dynamics of the molten contact line and its eventual arrest by freezing, and consequently are not in a position to answer the most fundamental question in molten droplet deposition: given the melt and target materials, how do we choose the droplet size and deposition conditions so as to produce a suitable solid shape? The answer to this question depends on the motion and arrest of the molten contact line.

ARREST OF A MOLTEN CONTACT LINE MOVING OVER A SUBCOOLED SOLID OF ITS OWN KIND: EXPERIMENTS AND THEORY

A molten droplet usually spreads over a cold substrate much quicker than it solidifies in bulk, that is, the drop remains essentially in liquid form until the contact line arrests. The point of contact line arrest determines the final shape of the droplet. An ordinary liquid's contact line arrests at a certain "equilibrium" contact angle. When a molten material is involved, however, the spreading is typically arrested by contact line freezing. Indeed, a little reflection shows that in homologous deposition (melt and target of the same material, one above and the other below the freezing point), there exists no meaningful final equilibrium contact angle.

Using an experiment where the rate of contact line advance was externally controlled, Schiaffino and Sonin (1997a) investigated the arrest of the contact line of a molten microcrystalline wax spreading over a subcooled solid "target" of the same material. They found (Fig. 1) that contact line arrest takes place at an apparent liquid contact angle which depends primarily on the Stefan number $S=c(T_f-T_i)/L$ based on the temperature difference T_f-T_i between the fusion point and the initial target temperature, c being the specific heat and L the latent heat of fusion. Neither the melt's superheat nor the prior history of the contact line motion appeared to significantly affect the contact angle at the point where the contact line comes to a halt.
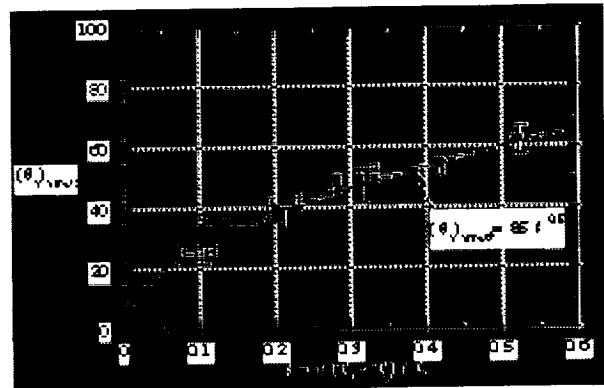

Figure 1 Apparent contact angle at arrest for microcrystalline wax

Schiaffino and Sonin proposed the following physical mechanism for contact line arrest due to freezing: arrest occurs when the liquid's dynamic contact angle approaches the angle of attack θ_s of the solidification front just behind the contact line (Fig. 2). Contact line advance is possible only as long as the liquid's contact angle θ_a exceeds θ_s.

In a second paper Schiaffino and Sonin (1997b) showed that the conventional continuum equations and boundary conditions for the slow spreading of a pure molten material over a solid of its own kind have no meaningful solution for θ_s. The quantity θ_s is deter-

[1] Professor, Department of Mechanical Engineering, Room 3-256, MIT, Cambridge, MA 02139; sonin@mit.edu
[2] Graduate Research Assistant, Department of Mechanical Engineering, Room 3-243, MIT
[3] Assistant Professor, Department of Mechanical Engineering, Room 3-158, MIT

mined by the heat flux just behind the contact line, and the heat flux in the conventional mathematical model is singular at the contact line. However, by comparing experimental data with numerical computations, Schiaffino and Sonin estimated that for microcrystalline wax, the breakdown of the conventional solidification model occurs within a distance of order 0.1-1 μm of the contact line. The physical mechanism for this breakdown is as yet undetermined, and consequently no first-principles theory exists at this time for θ_s and thus for contact line arrest. However, the functional relationship $\theta_s \approx f(S)$ can in principle be determined experimentally for each material.
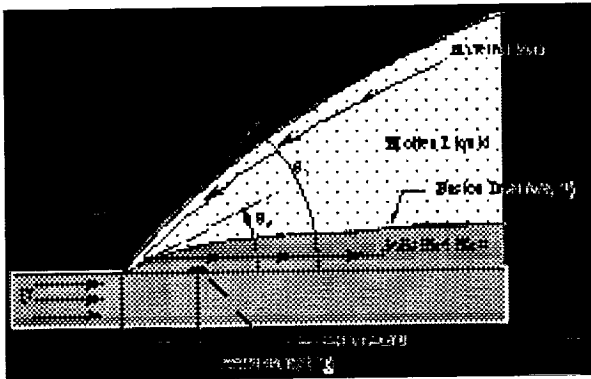

Figure 2 The near contact line region in the for a microcrystalline wax contact line reference frame.

MOLTEN DROPLET DEPOSITION: SIMILARITY LAWS AND EXPERIMENTS

A third paper by Schiaffino and Sonin (1997c) presents a study of the deposition process of molten droplets, from the instant of contact to complete solidification. This study lays down a framework for understanding low to moderate Weber number molten droplet deposition in terms of similarity laws and experimentation. The study is based on experiments with three molten materials—molten wax on solid wax, water on ice, and mercury on frozen mercury—which between them span a considerable range of the deposition/solidification similarity parameters. Based on experiments from the highly viscous limit to the inertia dominated limit, correlations are obtained for the spreading velocity, spreading time scales, the spreading factor (i.e. ratio of deposited drop's final footprint radius and the drop's initial radius), post-spreading liquid oscillation amplitudes and time scales, and bulk solidification time scales. At low to moderate Weber numbers, spreading is driven principally by

interfacial forces at the contact line rather than by impact phenomena. The main *dynamic* similarity parameter is the Ohnesorge number $Z=\mu/(\rho\sigma a)^{0.5}$, where μ is the absolute viscosity, ρ is the density, σ in the surface tension, and a is the drop radius. The principal similarity parameter for contact line arrest is the Stefan number.
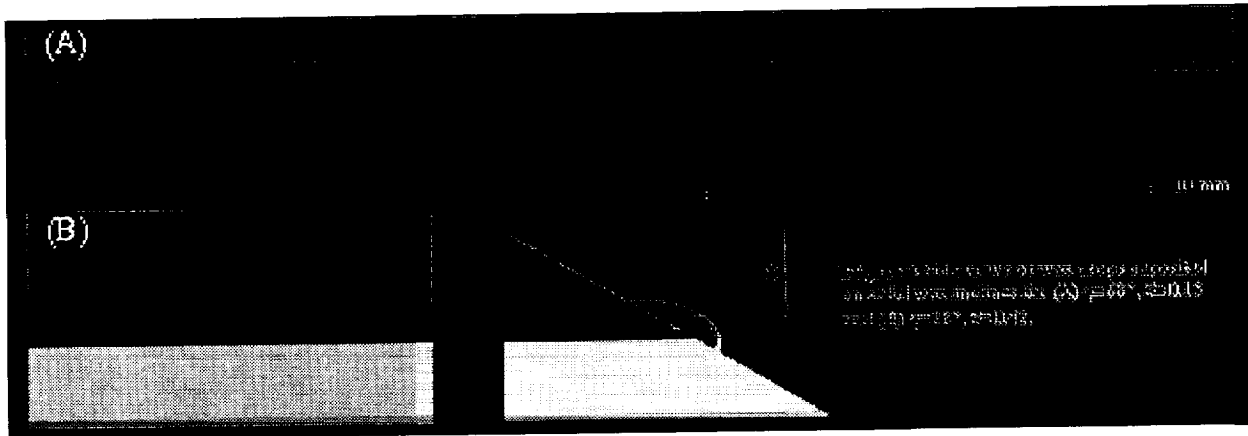
FURTHER EXPERIMENTS

Experiments have been carried out to (i) extend the investigation of contact line freezing to different materials and conditions, (ii) investigate the relationship between the dynamic contact angle and the contact line speed during spreading, and (iii) better define the thermal and solidification properties of the microcrystalline wax we have been using.

Contact line motion and arrest were studied by depositing molten drops with radius of order 1 mm on solid targets below the melt's fusion point, and photographing the process using high-speed video microscopy. Complete spreading, arrest and solidification events were recorded for molten wax on solid wax, for water on ice, and for molten wax deposited on inclined wax surfaces in order to investigate gravitational effects on molten contact line dynamics and arrest (Fig. 3). From the high-speed video data we obtain empirical relationships between the instantaneous values of the capillary number $Ca= \mu U/\sigma$ (U is the contact line advance speed) and melt contact angle θ_a. This relationship is discussed in the next section.

Post-arrest angles were obtained for molten solder on glass, molten solder on solid solder, and for octacosane on solid octacosane with two different (measured) surface roughnesses. Octacosane $(C_{28}H_{58})$ is a low melting point alkane with a distinct fusion point and latent heat release, and has well known thermal properties. We also investigated molten octacosane on clean glass and on glass coated with two types of self-assembled monolayers, one of which chemically resembles octacosane. These results will be discussed at the conference.

In addition, a study was completed of the thermal and solidification properties of microcrystalline wax, including its thermal conductivity k and enthalpy h(T) and specific heat c(T) at temperatures between 0°C and 115°C (Torresola, 1998). This wax has a distinct fusion point at 90° C (Schiaffino, 1996), but releases latent heat over a broad temperature range (about 20°C) below that point.

143

THEORY FOR VELOCITY VS. ANGLE AT A MOLTEN CONTACT LINE

A significant body of both experimental and theoretical work has built up over the past two decades on the relationship between speed and apparent contact angle at an *ordinary* liquid contact line. See for example the reviews by Dussan V. (1979), de Gennes (1985), Kistler (1993), Blake (1993), and the comments in Schiaffino & Sonin (1997a). One of the simplest approximate forms of this relationship is the Hoffman-Tanner-Voinov law for small Ca (Hoffman, 1975; Tanner, 1978; Voinov, 1976, 1978; see also Boender, et al, 1991),

$$Ca = \kappa\left(\theta_a^3 - \theta_m^3\right) \qquad (1)$$

where θ_m is the liquid's contact angle at the molecular scale, and is usually identified with the equilibrium angle. Hoffman's experimental value for κ is about 1.3×10^{-2} rad^{-3}, although it does in fact depend weakly on flow system size.

Other than some results mentioned in Schiaffino and Sonin (1997a), no work has previously been done on the Ca vs. θ_a relationship for a *molten* contact line. The molten dynamic contact line problem differs significantly from the ordinary one in that a solidification front forms underneath the molten material as it moves across the subcooled solid, and the material streamlines move into the solid as sketched in Fig. 2. Schiaffino & Sonin (1997a,b) argued that the solidification front at the contact line is wedge-like with a slope θ_s relative to the "horizontal", and deduced $\theta_s(S)$ empirically.

We have adapted Voinov's methodology to the molten contact line and obtained solutions for the liquid flow field near the contact line and for Ca vs. θ_a (Duthaler, 1998). Since the actual solidification front

shape near the contact line is unknown, we approximate it as piecewise continuous, with constant slope θ_s up to a cut-off distance $r=\lambda$ and zero slope thereafter (Fig. 4). The flow in the liquid region is assumed to be inertia-free and quasi-steady near the contact line, with viscous forces balancing the pressure gradient resulting from interfacial curvature. In general the equations require a numerical solution, but in the final stages of the arrest process, where $(\theta_a-\theta_s)<<\theta_s$, they yield the following surprisingly simple analytical expression

$$Ca = \frac{\kappa}{\sin\theta_s}\left[\left(\theta_a - \theta_s\right)^4 - \left(\theta_m - \theta_s\right)^4\right] \qquad (2)$$
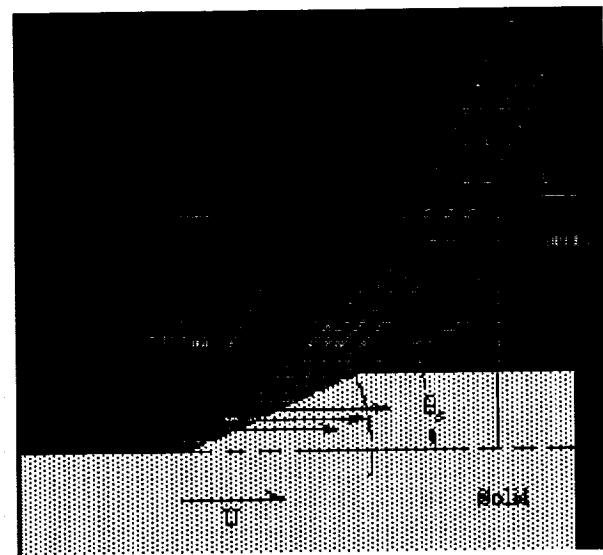

Figure 4 Piecewise continuous solidification front geometry used in modeling the molten dynamic contact line problem

Here, κ plays a role similar to the coefficient in Eq. (1), but does not have exactly the same value. Eq. (1) is in essence an analog of the Hoffman-Tanner-Voinov

law for molten materials approaching the final stage of arrest. Note that near contact line arrest, Ca scales as the 4th power of the (small) difference $\theta_a-\theta_s$. This behavior differs dramatically from that of the Hoffman-Tanner-Voinov Law, Eq. (1).

The theory can be applied, for example, to calculate the time scale associated with a molten drop spreading event. For example, in the limit of small Bond and Capillary numbers and small interfacial angles (θ_a,θ_m, $\theta_s<<1$), we obtain

$$\frac{1}{(\theta_a - \theta_s)^3} - \frac{1}{(\theta_0 - \theta_s)^3} = \frac{3\theta_s^{4/3}}{sin\theta_s}\frac{t}{\tau} \qquad (3)$$

where θ_0 is the value of θ_a at t=0,

$$\tau = \frac{\mu}{3\kappa\sigma}\left(\frac{4V}{\pi}\right)^{1/3} \qquad (4)$$

is a characteristic time, and V denotes the volume of the drop. Note that $\theta_a-\theta_s \sim t^{1/3}$ for this case. Applying a similar scaling analysis to Schiaffino's force feed experiment (see Schiaffino and Sonin, 1997b) shows that very near the arrest of a force fed droplet, $\theta_a-\theta_s \sim t^{-1/6}$.

The magnitude and trends predicted by the new spreading model are in basic agreement with our experimental results (Fig. 5). The plot shows empirical data for a drop deposition characterized by S=0.15, along with the predictions of various spreading models. The solid line represents the numerical solution of the new hydrodynamic equations derived for melts, based on applying Voinov's methodology to the simplified, wedge-like solidification interface of Fig. 4. We have set the wedge size λ equal to the cut-off distance computed by Schiaffino and Sonin (1997b), $\lambda\approx0.1$ μm. We also take $\theta_s=20°$, and assume that $\theta_m=\theta_s$ and that the bulk of the drop remains hemispherical during the final, slow stage of spreading. The approximate solution given by Eq. (2) with $\theta_s=\theta_m=20\bullet$ is shown using long dashes. Since no *a priori* model for θ_s exists, we choose the value $\theta_s=20\bullet$ to ensure good agreement with the experimental final arrest angle, 28.5•. For reference, Fig. 5 also shows Eq. (1) with θ_m set equal to the final arrest angle. At Ca<10^{-2} this equation overestimates Ca for given θ_a by nearly an order of magnitude.

HIGH-RESOLUTION MICROSENSORS FOR THE THERMAL PROCESSES NEAR THE MOVING CONTACT LINE

Before a useful theory for molten contact line advance and freezing can be developed, we need a realistic model for the heat flux at the contact line. One of
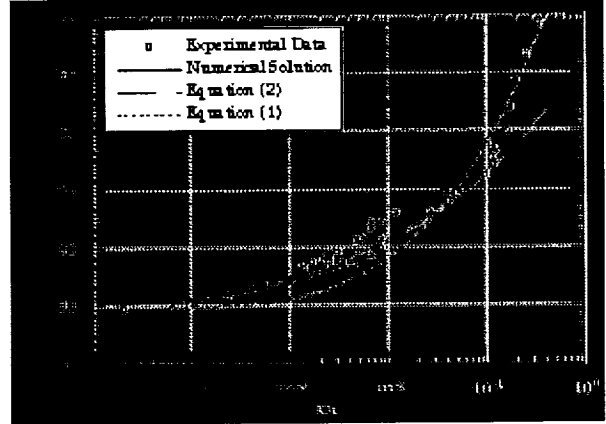

Figure 5 θ_a vs. Ca relationship for a molten drop of microcrystalline wax spreading over a solid target of the same kind. The numerical solution begins when R/a=1.64 and H/a=0.90.

the key objectives of our program is the development of micron-scale sensors for measuring the transient temperature at a point on the substrate surface as a molten contact line moves over it. The hope is that from this temperature history, we can back out information on the heat flux distribution near the contact line and obtain important clues about the nature of the thermal process in that region.

The sensors are of the thermistor type, microfabricated with silicon-based technology on either pure silicon or amorphous silicon dioxide wafers, 100 mm in diameter and 0.5 mm thick. Each wafer has room for 60 chips. Each chip has 32 sensors on its surface, 8 arrayed in a cross-pattern and spaced 400 μm apart, 8 arrayed in line with 200 μm spacing, and 16 arrayed in line with 50 μm spacing (Figs. 6 and 7). The sensors in the two coarsely spaced arrays are 2.5 μm square, and those in the fine array are 1.5 μm square. The time response is better than 10 μs. The sensing elements are made of boron-doped silicon and are electrically connected to the outside circuitry by aluminum circuit traces and gold wires. Temperature is sensed via Wheatstone bridges which detect the sensors' resistance variations due to temperature. Each individual sensor must be separately calibrated. Data is acquired with a PC 16-channel interface board, at a maximum rate of 10^6 samples/sec.

At the time of writing, the chips have been fabricated on wafers (we have several hundred chips of each of the two substrate materials), and a dozen chips have been cut and packaged. The data acquisition system has been constructed, and sensor calibration and testing is in progress. Some results on thermal

transients during contact line passage will be available for the August conference. While we expect that the data will provide information on the near-contact-line heat transfer process, we also foresee possible problems. First, small as they are, the sensors are actually slightly larger than the cutoff lengths computed by Schiaffino and Sonin (1997b), and the spatial resolution may be insufficient for resolving the near-contact-line region where the conventional model departs from reality. Second, due to the microfabrication method the conductors protrude about 0.5 μm above the substrate surface, which may be large enough to affect contact line motion. Finally, a sensor's temperature history will depend not only on the heat flux distribution into it from the fusion front, but also on the thermal properties of the substrate below it and the solidified melt between it and the fusion front (Fig. 2). The heat flux distribution in the contact line region must therefore be unfolded from computations of the overall system's transient response. Whether these potential problems are significant will become clear as the work proceeds.
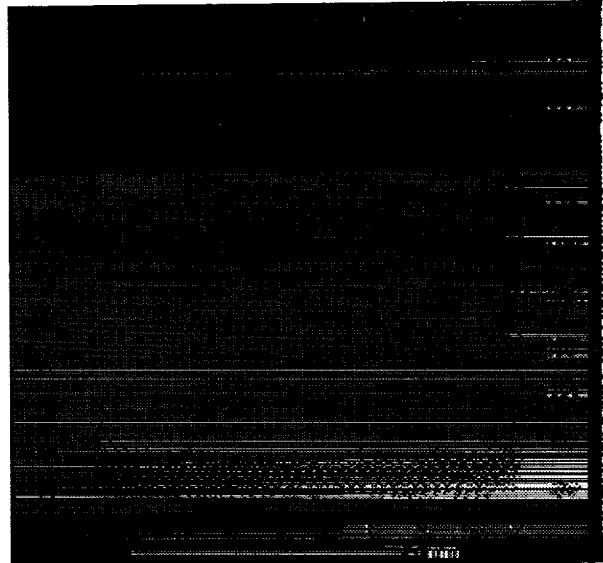
ACKNOWLEDGEMENTS

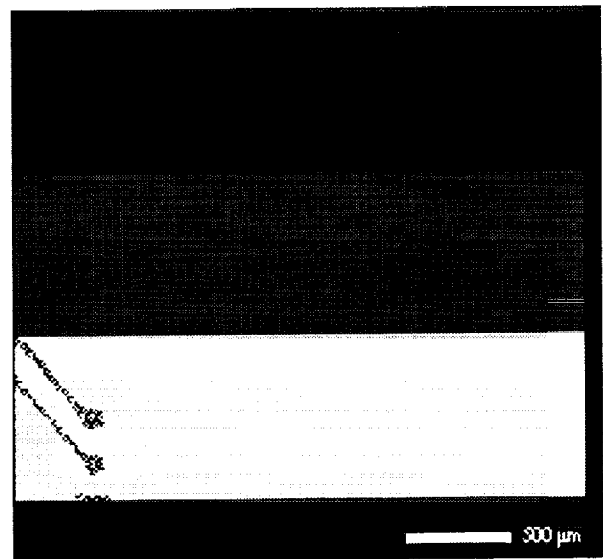Figure 6 Silicon thermal sensor chip showing the sensor arrays

Figure 7 Close-up of the coarse cross-pattern sensor array

146

REFERENCES

Blake, T. D., in *Wettability*, J. C. Berg, editor, Marcel Dekker, New York, 1993, 251-309.

Boender, W., A. K. Chesters, and A. J. J. van der Zanden, 1991, *Int. J. Multiphase Flow*, 17, 661-676.

de Gennes, P. G., 1985, *Rev. Mod. Phys.*, 57, 827-863.

Dussan V., E. B., 1979, *Ann. Rev. Fluid Mech.*, 11, 371-400.

Duthaler, G., Ph.D. Thesis, Department of Mechanical Enginering, MIT, in progress.

Gao, F. and A. A. Sonin, 1994, *Proc. Roy. Soc. London A*, 444, 533-554.

Hoffman, R. L., 1975, *J. Colloid and Interface Sci.*, 50, 228-241.

Kistler, S. F., in *Wettability*, J. C. Berg, editor, Marcel Dekker, New York, 1993, p. 311-429

Liu, Michael, MS Thesis, Department of Mechancial Engineering, MIT, in progress.

Schiaffino, S., 1996, *The Fundamentals of Molten Microdrop Deposition and Solidification*. PhD Thesis, Department of Mechanical Engineering, MIT.

Schiaffino, S., and A. A. Sonin, 1997a, *Phys. Fluids,.* 9, 3172-3187.

Schiaffino, S., and A. A. Sonin, 1997b, *Phys. Fluids.*, 9, 2217-2226.

Schiaffino, S. and A. A. Sonin, 1997c, *Phys. Fluids.*, 9, 2227-2233.

Tanner, L. H., 1979,*J. Phys D: Appl. Phys.*, 12, 1473-1484.

Torresola, J., 1998, Solidification Properties of Certain Waxes and Paraffins. MS Thesis, Department of Mechanical Engineering, MIT.

Voinov, O. V., 1976, Translated from Izvestiya Akademii Nauk SSSR, Mekhanika Zhidkosti i Gaza, No. 5, 76-84.

Voinov, O. V., 1978, *Sov. Phys. Dokl.*, 23, 891-893.